Bellerophontes: an RNA-Seq data analysis framework for chimeric transcripts discovery based on accurate fusion model

Francesco Abate[1,*], Andrea Acquaviva[1], Giulia Paciello[1], Carmelo Foti[1], Elisa Ficarra[1], Alberto Ferrarini[2], Massimo Delledonne[2], Ilaria Iacobucci[3], Simona Soverini[3], Giovanni Martinelli[3] and Enrico Macii[1]

[1]Department of Control and Computer Engineering, Politecnico di Torino, Torino 10129, Italy [2]Department of Biotechnology, Università di Verona, Verona 37134, Italy [3]Institute of Medical Oncology and Hematology, Università di Bologna, Bologna 40138, Italy

Associate Editor: Alex Bateman

ABSTRACT

Motivation: Next-generation sequencing technology allows the detection of genomic structural variations, novel genes and transcript isoforms from the analysis of high-throughput data. In this work, we propose a new framework for the detection of fusion transcripts through short paired-end reads which integrates splicing-driven alignment and abundance estimation analysis, producing a more accurate set of reads supporting the junction discovery and taking into account also not annotated transcripts. Bellerophontes performs a selection of putative junctions on the basis of a match to an accurate gene fusion model.

Results: We report the fusion genes discovered by the proposed framework on experimentally validated biological samples of chronic myelogenous leukemia (CML) and on public NCBI datasets, for which Bellerophontes is able to detect the exact junction sequence. With respect to state-of-art approaches, Bellerophontes detects the same experimentally validated fusions, however, it is more selective on the total number of detected fusions and provides a more accurate set of spanning reads supporting the junctions. We finally report the fusions involving non-annotated transcripts found in CML samples.

Availability and implementation: Bellerophontes JAVA/Perl/Bash software implementation is free and available at http://eda.polito.it/bellerophontes/.

Contact: francesco.abate@polito.it

1 INTRODUCTION

The analysis of RNA-Seq data revealed to be particularly effective for the detection of fused genes, which have been shown to be involved in several diseases. By applying RNA-Seq short reads, novel fusion genes and in particular the VAPB-IKZF3 chimera have been found to play a key role in the survival in breast cancer cells (Edgren *et al.*, 2011). In Maher *et al.* (2009), the analysis of single long reads has been performed to reveal novel fusion junctions. However, the application of short paired-end reads has been recently demonstrated to provide higher dynamic range and sensitivity in supporting fusion transcripts (Maher *et al.*, 2009). In paired-end
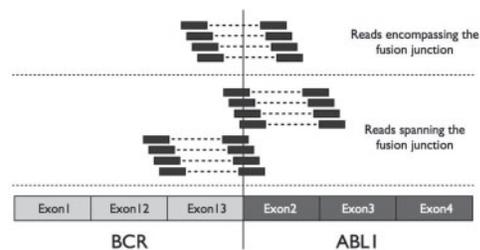

Fig. 1. Paired-end reads alignment on a gene fusion junction

reads, both the forward and reverse template strands of each DNA fragment are sequenced. The two sequenced ends, also known as the two 'mate' reads, are spaced by a gap of unknown nucleotides, whose size is approximately known.

The nature of the paired-end reads and the way they map on a gene fusion boundary offer the opportunity to detect possible chimeric candidates. Figure 1 shows a schematic representation of how the paired-end reads map on two fused genes. According to the reads arrangement over the fusion junction, two scenarios might occur as follows (i) each mate of the read encompasses the junction and maps on a different gene of the fused gene couple. The read is considered as a read 'encompassing' the fusion boundary; (ii) alternatively, a single mate of the read overlaps the fusion junction while the corresponding paired-end mate matches one of the two genes involved in the fusion. In this case, the read is considered as 'spanning' the fusion junction.

Encompassing reads can be used to find a first list of gene fusion candidates, while spanning reads are used to detect the exact boundary sequence. Since in the case of spanning reads the mate overlapping the junction breakpoint is discarded by conventional short reads aligners, these reads must be searched on the set of initially unmapped mates. These reads are then mapped on an artificially constructed putative fusion junction from candidate gene pairs previously detected through encompassing reads analysis.

In this work, we propose a new framework for the detection of fusion transcripts through short paired-end reads. With respect to currently available solutions, Bellerophontes provides the following contributions:

- To improve the quality and selectivity of fusion discovery, Bellerophontes selects those fusions matching an accurate

---

gene fusion model. The model, based on validated experimental evidence, is implemented by Bellerophontes through a set of modular filters.

- It integrates a splicing-driven alignment and abundance estimation analysis, leading to a more accurate set of reads supporting the junction discovery because it reduces ambiguous assignments of reads to isoforms and allows the detection of novel fused transcripts. Furthermore, this approach allows to account for those transcripts that are consistently expressed in the sample under study, even if they are not annotated.

- The full pipeline has been developed on top of a splicing-driven alignment. As a result, encompassing reads are mapped more accurately even in presence of proximal splice junctions. This enhances the accuracy of reads supporting fusion candidate detection and junction sequence discovery.

To achieve these targets, Bellerophontes leverages upon algorithms such as Cufflinks Trapnell *et al.* (2010) and TopHat Trapnell *et al.* (2009), aimed at overcoming RNA-Seq challenges concerning multiple read alignment, novel transcript discovery and accounting for alternative splicing. In addition, it exploits recent researches about the pattern of reads mapping across fusion breakpoints (Edgren *et al.*, 2011), enabling a more accurate model of the fusion junction. On this concern, Bellerophontes presents distinguishing features with respect to fusion detection tools proposed in the last year (Li *et al.*, 2011; McPherson *et al.*, 2011; Sboner *et al.*, 2010) http://tophat-fusion.sourceforge.net, in that it integrates these new instruments in a fusion detection software framework.

In this article, we report the fusion genes discovered by the proposed framework on experimentally validated biological samples of chronic myelogenous leukemia (CML) (Soverini *et al.*, 2011), and on public NCBI datasets of validated fusions. We also performed a comparative analysis with an alternative state-of-art approach (McPherson *et al.*, 2011) on the same datasets. The results highlight that Bellerophontes, while recognizing the validated fusions, reduced the final set of predictions and includes fusions involving non-annotated genes.

2 METHODS

2.1 Procedure and algorithms

This section first focuses on the computational infrastructure of the proposed tool and, then reports details about the application of the tool to real data analysis. The flow is mainly composed of two building blocks: 'chimeric candidates detection' and 'exact junction breakpoint analysis' (Fig. 2). 'chimeric candidates detection' aims at providing the list of possible chimeric candidates by detecting and analyzing those reads encompassing putative fusion junctions. 'exact junction breakpoint analysis' relies on the detection of the exact junction breakpoint between two gene candidates through the collection of reads spanning the putative junction breakpoint.

2.1.1 Chimeric candidates detection Figure 2a depicts the schematic flow of the chimeric candidates detection. This phase is composed of three steps: (i) Initial sample alignment to the genome reference; (ii) mapping of read mates to transcripts determined by abundance analysis and (iii) detection of the encompassing reads from the overall set.
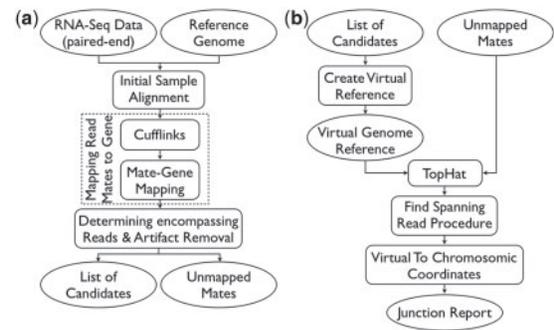

Fig. 2. Complete analysis flow schema of the proposed tool. (**a**) 'chimeric candidates detection and (**b**) 'exact junction breakpoint analysis'

Initial sample alignment. The starting point for determining the list of chimeric candidates is the alignment of short RNA-Seq paired-end reads to the reference genome (initial sample alignment). Most of fusion detection tools adopt Bowtie Langmead *et al.* (2009) for aligning paired-end reads to the reference genome. Conversely, we exploit the capability of TopHat alignment tool (Trapnell *et al.*, 2009) to align read fragments on a reference genome considering splicing events. TopHat reports variable length alignments due to the presence of splicing junction breakpoints. Consequently, the framework has to take into account spliced alignments to the reference genome instead of fixed length reads. At the end of the initial alignment of paired-end reads, both mapped (that include possible encompassing) and unmapped (that include possible spanning) reads are extracted.

Mate-gene mapping. In order to find out candidate genes involved in a fusion event, we need to assign the read location to an annotation file. In the 'mate-gene mapping' (see Fig. 2), we map each aligned mate on the transcripts detected by transcript abundance analysis by means of Cufflinks (Trapnell *et al.*, 2010), thus overcoming the limit of considering only known and annotated transcripts. In fact, analyzing RNA-Seq samples it is possible to reveal new alternative splicing events, novel genes and transcripts that might be neglected in an official annotation file. This is relevant in the context of chimeric transcripts, which are unpredictable events. In this context, a fusion possibly involves non-annotated genes or genes showing intron retentions. Considering only annotated gene isoforms, those reads encompassing the non-annotated region would be discarded and thus the fusion would not be detected.

Discordant mates detection and candidate filtering. The collected set of mapped read mates is analyzed in order to retrieve the subset of reads having the two mates mapping on different genes. At the end of the chimeric candidates detection phase, the list of possible gene candidates and the set of initially unmapped reads are provided.

On this set of candidates, a cascade of filters is applied to reduce the impact of errors due to the alignment phase as well as artifacts in the preparation of the biological sample (Edgren *et al.*, 2011). Moreover, ambiguous alignments due to paralogue or homologous regions are taken into account. Related filters will be discussed at the end of this section. As regards filters on artifacts, they are aimed at discarding: (i) reads that detect multiple couples of gene fusion candidates that, besides their discordant matching, they also have both mates on the same gene and (ii) reads showing an abnormal inner size (computed as described in Fig. 3) between the sequenced ends, or asymmetry in the alignment of the mates encompassing a fused gene (an example is shown in Fig. 4).

We focus now the discussion on the this second type of filter, namely, the 'abnormal inner size filter', which implements a strategy similar to Sboner *et al.* 2010, where the distribution of the inner distances in the sample is computed and outliers are removed based on a threshold. In this work, this has been set to 400 bp. In Bellerophontes, inner distance is computed through consensus regions as depicted in Figure 3. This is a minimum inner distance,
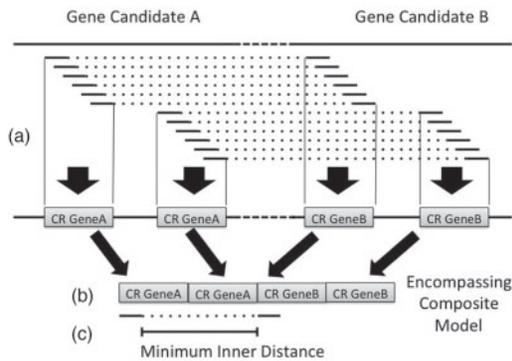
Fig. 3. Consensus regions and inner distance computation. (**a**) For each encompassing read mate the consensus is computed. (**b**) Then, all the consensi are unified and composed into a single composite model representing the isoform determined by the encompassing reads. (**c**) The inner distance is computed as number of base pairs corresponding to the composite model counted from the end of the first mate to the start of the second mate
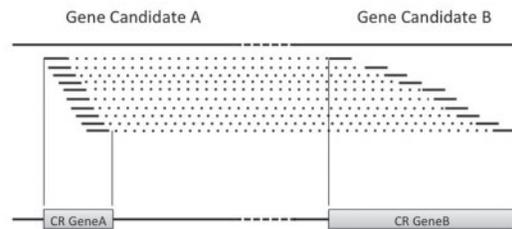

Fig. 4. Asymmetric abnormal fusions. Example of abnormal fusion. The gene candidate B presents a consensus that is widely larger than the partner

because the consensus regions are made by encompassing reads and for this reason they may not be complete, as reads spanning the junction in this phase of the pipeline are not considered. As such, the inner distance is in general larger than the sum of the consensi determined through encompassing reads.

In this work, we also propose a new and extended implementation that takes into consideration a recent observation in Edgren *et al*. (2011) about the asymmetry in the alignment. This is recognized to be a feature of artifacted chimeric transcripts.

This filter looks at consensus regions made by encompassing reads on the candidate genes. The length of these regions is computed (excluding possible gaps in between) as shown in Figure 3. If one of the two regions, for instance the one related to Candidate A in Figure 4, is much larger than the corresponding consensus region of the Candidate B, the couple A–B is discarded.

After filtering the reads involved in artifacts and alignment errors, another set of filters on chimeric candidates is performed. Candidates supported by a percentage of ambiguous reads with respect to the total number of reads are discarded (see Table 3 in Section 3 for details). Ambiguous reads are caused by short or long homologous sequences in the reference genome. Fusion detection analysis is affected because the mate pairs that, without homologous sequences, would match on the same gene, match discordantly on two distinct but similar genes, thus creating fake encompassing reads. Homologous regions may be due both to the presence of paralogue genes that share long sequence regions and to the presence of short similar sequences.

The 'homologous sequence artifacts filter' implements two different policies for both cases. Concerning the long homologous sequences due to paralogue genes, a filter that query TreeFam (Li *et al*., 2006) database

has been implemented. For short homologous sequences, we apply a strategy similar to what proposed in Sboner *et al*. (2010), where read mates encompassing the fusion candidates are extracted and reversely mapped on the same genes.

The remaining filters look at gene candidate distance and number of supporting encompassing reads. In particular, fusions occurring between genes closer than a user defined threshold are filtered out by the 'neighbor candidate filter', as they are considered instances of transcriptional readthroughs (Edgren *et al*., 2011). Finally, since both alignment bias and biological sample preparation artifacts produce false fusion candidates that are typically supported by a small number of encompassing reads, chimeric candidates having the number of encompassing reads below a user-defined threshold are filtered out by the 'supported candidates thresholding filter. The threshold value depends on the coverage of the overall sequencing experiment and adopted protocol.

2.1.2 Junction breakpoint analysis Starting from the list of fused candidates previously detected, the scope of the exact junction breakpoint analysis phase, outlined in Figure 2b, is to determine the exact junction breakpoint and validate the gene fusion by the alignment of unmapped reads to the putative junction.

From a computational point of view, the problem of finding gene fusion junctions can be considered an extension of the detection of splicing events involving exons couples belonging to different genes and chromosomes. Splicing events introduce a considerable level of complexity in the analysis of RNA-Seq fragments. Intron regions cause many mismatches, making alignment programs to fail across the junction. Splicing discovery programs (Ameur *et al*., 2010; Bryant *et al*., 2010; Trapnell *et al*., 2009) are aimed at efficiently detecting the exact intron–exon boundary. Due to the considerable computational complexity, they limit their research within a maximum intron size.

To exploit the junction discovery capabilities of splicing detection tools without compromising computational efficiency, exact junction breakpoint analysis adopts a virtual reference: (i) for each couple of gene candidates, a virtual reference consisting in the concatenation of the two genes is created and (ii) a splicing discovery algorithm (i.e. TopHat) is launched on the virtual reference providing as input the initially unmapped reads resulting from the 'chimeric candidates detection phase'.

As shown in Figure 2b, in order to create a 'virtual fusion junction' a 'create virtual reference' module automatically retrieves the sequences corresponding to the gene fusion candidates using the coordinates provided by Cufflinks. The corresponding sequence is retrieved from the reference in 'UCSC Genome Browser database' (Fujita *et al*., 2010). Being based on Cufflinks coordinates, the sequences retrieved on the reference may correspond to annotated or non-annotated genes.

The sequences are then concatenated and the resulting file represents the virtual genome reference of the virtual fusion junction. TopHat receives as input the set of unmapped reads and the virtual genome reference, resulting from the concatenation of the two gene fusion candidates. The result of TopHat is a file containing all the mapping reads including the spanning end mates. After TopHat alignment, a rearrangement from virtual to chromosomal coordinates is needed.

Once the set of end mates spanning, the gene fusion junction is collected and the read coordinates are translated from virtual to genomic 'coordinates', it is possible to exactly determine the boundary junction among the two gene candidates. As shown in Figure 5, end mate reads spanning the gene fusion junction can be represented as a split read and each chunk maps on a different gene section. It is worth noting that all the spanning mate chunks are spaced by a gap in the genome reference. The exact points where the first mate chunk ends and the second mate chunk starts represent the exact junction boundary coordinates.

In conclusion, at the end of the exact junction breakpoint analysis for each couple of gene fusion candidates, the set of putative junctions as well as the supporting spanning reads are reported. However, the detection of spanning reads can be affected by propagation errors due to both alignment
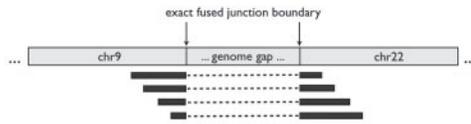
Fig. 5. Schematic representation explaining how spanning mates reveal exact genome coordinates of gene fusion junction. Spanning mates are indicated as black solid lines separated by a dashed line in correspondence of the junction breakpoint
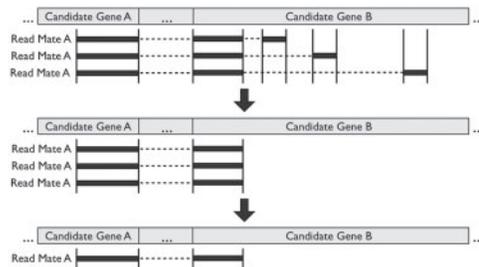

Fig. 6. Floating fragment removal filter. Some subsequence of the same Read Mate A maps differently on the two Candidate Gene A and B. Specifically a small fragment floats along the Candidate Gene B. The floating fragment removal filter removes the floating fragments considering as a valid mapping only the subsequences commonly mapped to the reference. Finally, only a single instance of read mapping is reported

limitations and artifacts in the experimental preparation of the sample. For this reason, the resulting junctions are analyzed and filtered depending on how the spanning read maps on each junction. Next section describes the filtering policy applied to improve the accuracy of the junction detection.

2.1.3 Spanning read analysis and junction filtering   The exact junction breakpoint analysis provides a list of putative junctions boundaries between two fused genes. A selection is performed at this stage by looking at the distribution of the reads spanning the junction, to reveal possible artifacts. Therefore, we apply some filters in order to remove all the artifact junctions from the resulting set and to make junctions list more accurate.

It might occur that the same read mate maps on the putative junction in multiple ways. In fact, some subsequences of the gene sequence might be homologous and consequently some small fragments of the read mate match the candidate gene in multiple places of the sequence. Thus, these fragments float on multiple places of the gene sequence and the accuracy of their mapping may be compromised. Furthermore, when this scenario occurs, TopHat reports a distinct read mate instance for each multiple match. However, this does not lead to a realistic count of the number of read mates supporting the junction.

To address this issue, we propose 'Floating Fragment Removal Filter' that removes all the small floating fragments of the read mate sequence mapping on multiple places of the reference gene. Figure 6, on the upper part, shows an example where the second mate is characterized by fragments mapping on different locations. Specifically, this filter detects and preserves all those read mate subsequences mapping the reference in the same region (see the middle part of Fig. 6). In this way, only those read portions that are highly probable to be correctly mapped on the reference sequence are considered to support the putative junction. Moreover, as only the commonly mapped subsequences are preserved, it is pointless to report multiple instances of the same read mate, therefore the mate is considered as a unique (see bottom part of 6).

A second filter, named PCR artifacts removal filter, is based on the observation that PCR amplification might cause false-putative junctions
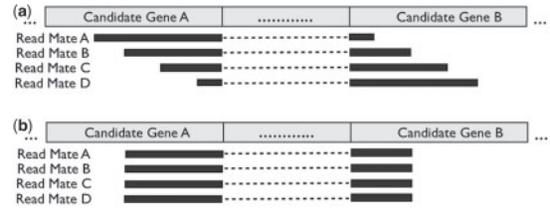

Fig. 7. PCR artifact removal filter. (**a**) The schema of a group of read mates spanning a genuine fusion junction. The short reads present a ladder-like pattern and they all map on distinct points of the candidate genes involved in the fusion. (**b**) An example of a group of read mates mapping a false breakpoint junction. Short reads are more overlapped as all the reads share a similar start and end mapping locations

(Edgren *et al*., 2011). Reads mapping exactly to the same position are likely due to an artifact originated by amplification and sequencing of the same initial fragment repeated more times. As a result, multiple identical reads are considered as a single one and the fusion supported by those reads will be discarded unless other supporting spanning reads will be found.

Since Cufflinks performs a transcript abundance analysis to detect the transcripts on which we map each aligned mate, reads duplication could affect the correct detection of the genes involved in the fusion as well as its junction breakpoint. We avoid the problem through the PCR artifact removal filter. Real fusions are characterized by a ladder-like pattern of the spanning reads supporting the junction (Fig. 7a). Conversely, false-positive junctions due to PCR amplification artifacts lack this pattern and all the short read mates spanning the junction either map on the same position or are one or two bases shifted (Fig. 7b). The PCR artifacts removal filter removes all those putative junctions lacking the ladder-like pattern.

A final filtering is performed on as follows (i) candidate fusions supported by a number of spanning reads lower than a user defined threshold (supported junctions thresholding filter) and (ii) coherency with encompassing reads. In particular, the latter is based on the observation that, in presence of a genuine gene fusion, the genomic coordinates of the set of encompassing reads must be adjacent or in some cases overlapped to the location of the spanning reads. Bellerophontes creates a consensus of the final set of both encompassing and spanning reads and checks if the coordinates of the corresponding locations are either adjacent of overlapped. If this check is negative, the fusion candidate is discarded.

2.2   Real data analysis

2.2.1 Materials and sample preparation   We present result about the detection of chimeric transcripts on three datasets at different stages of CML progression from a Philadelphia chromosome-positive (Ph+) CML patient (sample s_4, s_7 and s_8; Soverini *et al*., 2011). The patient was diagnosed with Ph+ p210BCR-ABL-positive CML by chromosome banding analysis. The samples were tested for rearrangements between BCR and ABL genes by reverse transcription–polymerase chain reaction (RT–PCR; Dongen *et al*., 1999).

RNA-Seq libraries (one per sample) were prepared using the mRNA-Seq 8 sample preparation kits following the manufacturer's instructions. We modified the gel extraction step by dissolving excised gel slices at room temperature to avoid underrepresentation of AT-rich sequences (Quail *et al*., 2009). Library quality control and quantification were performed with a Bioanalyzer Chip DNA 1000 series II (Agilent). Libraries were sequenced on an Illumina genome analyzer II following the manufacturer's instructions and 75 bp paired-end reads were obtained.

The second dataset we used for evaluation is a public sets of RNA-Seq data including information about RT-PCR validated fusions [Berger *et al*., 2010], obtained from NCBI database (http://www.ncbi.nlm.nih.gov/sra) under submission numbers SRA009053 and SRA040160.

Table 1. Fusions predicted with Bellerophontes on chronic myelogenous leukemia samples

Lib.	[#] Reads (Mlns)	Read Len.	Frag. Mean	Frag. Stdev	Total Fus.	Inter Chr.	Intra Chr.
s_4	20	75	212	16	2	2	0
s_7	32	75	225	19	4	3	1
s_8	29	75	229	22	10	9	1

Table 2. Fusions predicted on publicly available RNA-Seq data

Library	Reads [#] (millions)	Read length	Fragment length	Validated predicted fusions
018259	14	50	500	1
018260	16	50	500	2
018261	16	50	500	1
018265	8	50	500	1
018266	15	50	500	4
018267	15	50	500	2
018269	15	50	350	3
NCIH660	7	50	NA	1

*All the library identifiers, with exception of the last row, refer to the accession number reporting the SRR prefix in the NCBI databank.

2.2.2 Fusions detected on real samples For both CML samples and NCBI datasets, we report the number of detected fusions. For all the reported analysis Bellerophontes ran with *GCCh37/hg* February 19, 2009 assembly of the human genome, while we used GRCh37 file for annotations from Ensembl.

Table 1 reports the statistics concerning all the CML samples and details about the number of total fusions detected. In all the samples, Bellerophontes detects the exact sequence of the chimeric fusion. In the last column, the number of intra chromosomic fusions are shown. Filter parameters used for these runs have been set as follows. Minimum supporting reads: 8; neighbor candidates filters: 500 000 bp; inner distance threshold: 400 bp.

Under the hypothesis that the scientist is not interested in adjacent fused genes (Edgren *et al.*, 2011), that can be detected by classical splicing detection tools, we set the neighbor candidates filters with 500 000 bp thresholds and this caused most of the revealed fusions to be inter-chromosome.

Table 2 highlights the capability of Bellerophontes concerning the detection of validated fusions on a published dataset. These samples have lower coverage (at most 16 million reads) and smaller read length (50 bp) compared with CML data (see Table 1 for comparison). All the 14 fusions validated in the seven samples of melanoma cells (Berger *et al.*, 2010) and the TMPRSS2/ERG fusion (causally linked to prostate cancer) in NCIH660 (Sboner *et al.*, 2010) have been successfully detected. For the analysis of NCBI samples, some filter constrains have been set to be less stringent with respect to CML samples, because of the specific characteristics of NCBI dataset in terms of coverage and presence of readthroughs. In particular, the threshold on the number of encompassing in the supported candidate thresholding filter was set to 2, since a lower coverage may cause a smaller number of supporting encompassing reads (see Table 5). Furthermore, the threshold for the neighbor candidate filter was set to 50 bp to account for the larger number of readthroughs in this dataset.
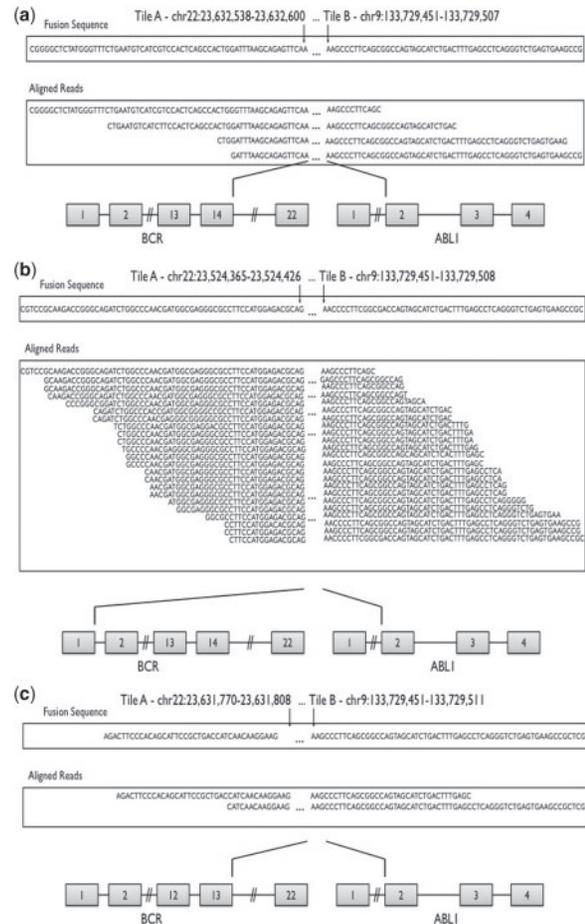

Fig. 8. Junction boundary detection. Results of the exact junction breakpoint analysis applied to CML samples. The fusion sequence corresponding to *BCR* and *ABL1* genes is reported as well as the group of reads spanning the junction boundary. The exons involved into the fusion are also indicated in correspondence of the fusion boundary points

2.2.3 Exact junction discovery details Figure 8 depicts the results of the exact junction breakpoint analysis applied to CML samples. A group of reads is mapped onto the reference genome spanning the fusion boundary between the *BCR* and *ABL1* genes. This chimera has been validated through RT–PCR analysis. The spanning reads reported in Figure 8 show a ladder-like pattern across the junction boundary according to the junction model we use in this work. The exons involved in the fusion are exon 14 (*s_4*), exon 1(*s_7*) and exon 13 (*s_8*) of *BCR* and exon 2 of *ABL1*.

Fusions involving non-annotated genes Using transcript expression analysis instead of annotated genes, Bellerophontes is able to detect fusions involving non-annotated genes. The analysis of Sample *s_8* reveals that 3 of 10 fusions involved non-annotated transcripts. For instance, Bellerophontes identifies a fusion involving *EWSR1* gene (chr22:29664273-29669806) and a not annotated gene (namely, CufflinksNovelGene chr14: 36350337-36350395). This feature is relevant for the detection of new aberrant modifications in the gene regulation, which is one of the main targets of next-generation sequencing analysis.

3 RESULTS

In this section, we report details about the effects of filters and the results about a comparative analysis with another recently published

Table 3. Effects of Bellerophontes filters

Lib.	Initial Cand.	Supp. Cand. Thrs.	Naming Incoher. (*)	Neigh Cand.	Abnormal Inner Dist.	Finally not filtered	Not filt. (%)
s_4	24 337	87%	8%	6%	34%	1754	7%
s_7	86 552	94%	13%	9%	36%	2482	3%
s_8	122 931	95%	19%	8%	41%	2791	2%

*Naming incoherencies are detected when the same gene name share different gene identifier in Cufflinks annotation. Thus two apparently different genes are actually a single gene.
The reported percentages are computed as the ratio between the number of filtered candidates and the number of candidates filtered by the previous filter

approach (McPherson *et al.*, 2011), which has been used to discover gene fusions in tumour samples (Steidl *et al.*, 2011).

3.1 Filtering effects

We detail the effects of the various filters applied both to the candidate fusions and to the spanning reads. We report filtering results of only the CML samples, but similar considerations can be drown for NCBI samples. Table 3 shows the effect of filters on candidate fusions (Section 2.1.1) while Figure 9 refers to spanning reads filtering. Numbers in the tables report the percentage of candidates removed with respect to the previous filter in the cascade.

3.1.1 Effects of filters on candidate fusions The considerable number of initial candidates detected in the first phase by discordant read mapping (up to 122 931 in *s_8* sample) is consistently reduced through the pipeline of filters shown in Table 3. A large fraction of candidates is discarded because it was not supported by a sufficient number of encompassing reads (see third column in Table 3). Moreover, 32%–37% of putative fusions with a sufficient number of encompassing reads has been removed because of abnormal inner size and asymmetry in consensus regions.

Because of its large computational cost due to the reverse remapping of the encompassing reads, the homologous sequence artifacts filter has been applied as a final step on a reduced set of candidates. This filter was very selective, leaving 3%–8% of putative candidates for the following spanning analysis phase.

3.1.2 Effects of filters on junction artifacts Both alignment bias and biological artifacts due to PCR amplification might cause the detection of false putative junctions. In order to mitigate the negative effects of these events on the chimeric transcript analysis, the filters described in Section 2.1.3 are applied during the exact junction breakpoint analysis phase. Figure 9 reports the effect of the application of the filters on the initial number of putative junctions detected for each sample. The initial number of junctions (i.e. spanning reads) is in general larger than the candidates resulted from the first encompassing analysis phase of the tool, since each candidate has multiple spanning reads associate to it.

The floating fragment removal filter does not reduce the number of the initial putative junctions. However, it plays a fundamental role for the following PCR artifacts removal filter. In fact, the floating fragments cause false ladder-like patters that are actually replicas of the same reads (see Fig. 6). The floating fragment removal filter removes the floating fragments and it allows a more accurate
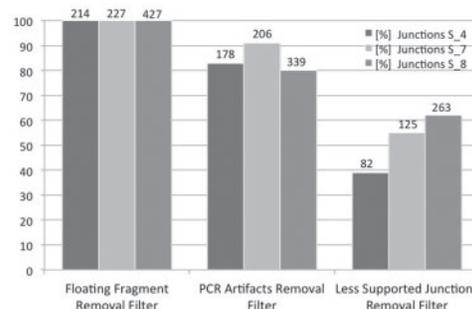

Fig. 9. Effects of the filters on the putative junctions. Percentage of putative junctions after the cascade of the filters on initially putative junction detected for the biological sample. The number of junction after the application of each filter is reported on the top of each histogram column

detection of PCR artifacts. Therefore, the PCR artifacts removal filter removes from the 9 to 20% of false putative junctions and the number of junctions ranges in the best case (sample *s_8*) from 427 to 339. Moreover, the removal of the floating fragments makes in some cases to considerably decrease the number of reads spanning across the putative junction (see Fig. 6). Consequently, the 'supported junctions thresholding' filter is more effective after applying floating fragment removal filter and the reduction spans from 39 to 62%.

3.2 Comparative analysis

To highlight that the proposed approach provides results comparable with state-of-art tools while it introduces original features improving fusion discovery, we compared Bellerophontes analysis with deFuse (McPherson *et al.*, 2011) on both CML samples and a published dataset. This represents a very recent fusion detection tool using paired-end reads. Its basic version has been shown to improve other tools such as FusionSeq (Sboner *et al.*, 2010) and MapSplice (Wang *et al.*, 2010) in detecting experimentally validated fusions. We applied deFuse version 0.4.2 with defaults options for the analysis on CML samples. We also compare public results in McPherson *et al.* (2011) with our results on the NCBI datasets.

Table 4 shows the final number of fusions predicted with Bellerophontes and deFuse on CML samples. This table also reports the number of encompassing and spanning reads for *BCR-ABL1* fusion (validated through RT–PCR). The number of predicted fusions by deFuse is higher for all the samples. While implementing more selective filters Bellerophontes still detects *BCR-ABL1* with a comparable number of encompassing and spanning. We note that there are several deFuse-unique fusions that are supported by a low number of spanning reads (i.e. <8). Those fusions are discarded by Bellerophontes because of the supported candidate thresholding filter, whose threshold was set to 8.

The smaller number of predicted fusions is also due to the usage of Cufflinks to map the discordant read mates. Indeed, only candidates with a minimum level of abundance are considered, reducing the set of possible fused genes to be evaluated in the successive stages of the pipeline. Indeed, we observed that most of the candidates provided by deFuse have been discarded by Bellerophontes because the related genes are filtered out by Cufflinks with default parameters, due to their low abundance. Note that, if we are interested in detecting junctions between poorly expressed candidates, it is possible to run Cufflinks with less restrictive

Table 4. Comparison between Bellerophontes and deFuse CML Data

Lib.	deFuse Tot.	Bellero Tot.	deFuse Enc.	Bellero Enc.	deFuse Span.	Bellero Span.
s_4	21	2	15	14	5	4
s_7	46	4	48	36	46	35
s_8	52	10	9	7	1	2

parameters. Note also that the set of candidates given by deFuse is not a superset of our candidates, this means that we find some candidates, that deFuse does not find, having a relevant expression. To quantify the impact of Cufflinks, we performed experiments with relaxed parameters. We observed an increasing number of fusions in common with deFuse, up to 85%. We do not state that these additional fusions are false positives. Rather, we believe that it is of interest of the biologist to be able to distinguish between fusions involving more or less expressed transcripts, because this may be correlated with protein expression analysis.

The number of encompassing and spanning reads in *s_4* sample is comparable for both the tools, whereas for the *s_7* sample deFuse presents an higher coverage. This is mainly due to the different alignment programs (Bowtie for deFuse and TopHat for Bellerophontes) and to the usage of Cufflinks transcript annotations in the proposed pipeline. In particular, our alignment and annotation methodology reduces the probability of multiple matches, which may lead to candidates with higher read coverage but not really expressed.

On the other side, considering results in Table 5, in case of fusions ANKHD1-C5orf32 (sample 018260), C1orf61-CCT3 and MIXL1-PARP1 (sample 018266), we observe a larger number of spanning reads supporting the validated junction. The number of spanning reads strongly depends on the splicing detection algorithm. Bellerophontes integrates TopHat in its pipeline, which allows to improve the quality of spanning reads detection. This becomes evident especially in case of junctions where deFuse shows a poor spanning reads coverage. For instance, in the case of sample *s_8* (see Table 4) of CML dataset and sample 018260 (see Table 5), the number of Bellerophontes detected spanning is considerably higher compared to deFuse. This result is coherent with the experimental validation [the fusion in the 018260 sample is validated with RT–PCR (Berger *et al.*, 2010)].

4 DISCUSSION

The proposed framework implements a new analysis pipeline that exploits effective alignment and annotation algorithms as well as a filtering stage based on an accurate modeling of the junction. RNA-Seq data analysis presents major challenges concerning ambiguous assignments of reads to isoforms that can impact fusion detection. Indeed, fusion candidates are discovered by means of encompassing reads. As such, the accuracy in detection of discordant mates is a key feature of a fusion detection pipeline. Bellerophontes introduces a new approach where reads are mapped on experimental determined transcripts rather than using a reference genome, thus reducing the probability of multiple matches that may affect state-of-art fusion detection tools based on basic alignment algorithms.

Table 5. Comparison between Bellerophontes and deFuse on publicly available data

Library*	5′ Gene	3′ Gene	deF. Enc.	Bel. Enc.	deF. Span.	Bel. Span.
018259	KCTD2	ARHGEF12	4	4	1	2
018260	ITM2B	RB1	19	17	2	2
018260	ANKHD1	C5orf32	2	7	2	23
018261	GCN1L1	PLA2G1B	4	3	1	1
018265	WDR72	SCAMP2	3	2	2	1
018266	C1orf61	CCT3	54	37	17	25
018266	MIXL1	PARP1	2	5	1	4
018266	C11orf67	SLC12A7	43	40	24	22
018266	GNA12	SHANK2	29	23	9	6
018267	TLN1	C9orf127	3	14	1	1
018267	ALX3	RECK	4	21	6	6
018269	ABL1	BCR	91	89	14	12
018269	NUP214	XKR3	67	58	15	16
NCIH660	TMPRSS2	ERG	19	23	10	11

*All the library identifiers, with exception of the last row, refer to the accession number reporting the SRR prefix in the NCBI databank.

A similar effect can be noted on the analysis of spanning reads supporting the junctions. By taking splicing events into consideration, Bellerophontes obtain a more robust detection of the exact junction sequence, which becomes evident especially where the number of supporting reads is poor. Note that the number of encompassing and spanning reads represent a discriminatory factor to conduct a successive experimental validation of the data provided by the software analysis.

The improved accuracy revealed another positive effect, that is the final number of detected fusions, even in the most covered libraries (*s_7* and *s_8*), is compatible with a cost sensitive experimental validation. Moreover, in *s_8* three fusions involving non-annotated genes are detected.

To improve selectivity, the pipeline integrates a set of filters, embedding a new and more effective junction model. Indeed, this filter discards a large number of candidates. Finally, results about spanning read filtering and spanning-encompassing coherence check highlight that a junction filtering is a critical step to provide an accurate set of junctions.

Note that in all the CML samples Bellerophontes was able to detect the expected and validated *BCR–ABL1* fusion even in a selective filtering context.

Comparative results obtained on both CML and NCBI dataset show that Bellerophontes is able to accurately detect gene fusions and improves the accuracy of spanning reads with respect to deFuse. This cross-benchmarking was performed since deFuse presented the most complete biological validation and it has shown to improve state-of-art tools like FusionSeq (Sboner *et al.*, 2010). The results indicate that deFuse is not able to detect chimeric transcripts involving non-annotated genes present in *s_8*. On the other side, Bellerophontes is much more selective, reducing the total number of fusion candidates with respect to deFuse (see Table 4).

Bellerophontes is based on pair-end reads. Other recently proposed approaches such as FusionMap (Ge *et al.*, 2011) exploit long single-end reads spanning the junction. Compared to FusionMap, our framework includes the support for new transcripts and the accurate mapping in presence of alternative splicing events.
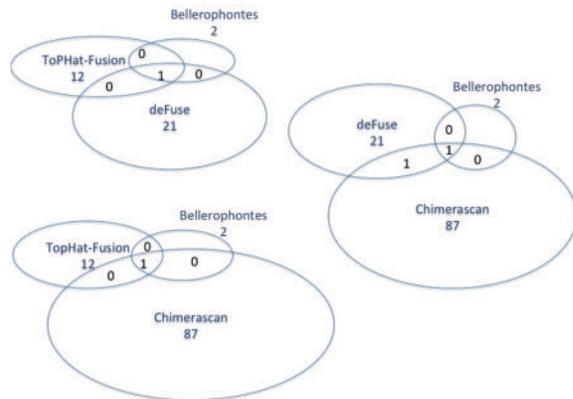
Fig. 10. Overlapping of the fusions detected by Bellerophontes, deFuse, Chimerascan and TopHat-Fusion on the sample CML *s_4*

We also performed a comparative analysis of Bellerophontes against deFuse, TopHat-Fusion (http://tophat-fusion.sourceforge. net) and Chimerascan (Iyer *et al.*, 2011), on the CML samples. All of them recognized *BCR–ABL1* and provided a set of additional fusions. Interestingly, there was almost no overlap among all the tools in respect of these additional fusions (Fig. 10). For this reason, most of them are likely to be false-positive. It can be noted that Bellerophontes has the smaller set of this additional fusions. Finally, we in order to further evaluate the performance of the proposed method we performed analysis on an additional dataset, that is *MCF7* cell line by Edgren *et al.* (2011), for which we found all the validated fusions, namely, BCAS4-BCAS3, ARFGEF2-SULF2 and RPS6KB1-TMEM49.

5 SOFTWARE

Bellerophontes is implemented in Java/Perl/Bash language. It runs on a standard Linux machine and it fully supports multithreaded computation. The performance strongly depends on the memory and number of CPUs available. However, the analysis on the proposed datasets have been performed with an Intel I7 TM920 at 2.67 GHz and 16 GB of RAM Memory.

Conflict of Interest: none declared.

REFERENCES

Ameur,A. *et al.* (2010) Global and unbiased detection of splice junctions from RNA-seq data. *Genome Biol.*, **11**, R34.

Berger,M.F. *et al.* (2010) Integrative analysis of the melanoma transcriptome. *Genome Res.*, **20**, 413–427.

Bryant,D.W. *et al.* (2010) Supersplat–spliced RNA-seq alignment. *Bioinformatics*, **26**, 1500–1505.

Dongen,J.J. *et al.* (1999) Primers and protocols for standardized detection of minimal residual disease in acute lymphoblastic leukemia using immunoglobulin and T cell receptor gene rearrangements and TAL1 deletions as PCR targets: report of the BIOMED-1 CONCERTED ACTION: investigation of minimal residual disease in acute leukemias. *Leukemia*, **13**, 110–118.

Edgren,H. *et al.* (2011) Identification of fusion genes in breast cancer by paired-end RNA-sequencing. *Genome Biol.*, **12**, R6.

Fujita,P.A. *et al.* (2010) The UCSC Genome Browser database: update 2011. *Nucleic Acids Res.*, **39**, D876–D882.

Ge,H. *et al.* (2011) FusionMap: detecting fusion genes from next-generation sequencing data at base-pair resolution. *Bioinformatics*, **27**, 1922–1928.

Iyer,M.K. *et al.* (2011) ChimeraScan: a tool for identifying chimeric transcription in sequencing data. *Bioinformatics*, **27**, 2903–2904.

Langmead,B. *et al.* (2009) Ultrafast and memory-efficient alignment of short DNA sequences to the human genome. *Genome Biol.*, **10**, R25.

Li,H. *et al.* (2006) TreeFam: a curated database of phylogenetic trees of animal gene families. *Nucleic Acids Res.*, **34**, D572–D580.

Li,Y. *et al.* (2011) FusionHunter: identifying fusion transcripts in cancer using paired-end RNA-seq. *Bioinformatics*, **27**, 1708–1710.

Maher,C.A. *et al.* (2009) Transcriptome sequencing to detect gene fusions in cancer. *Nature*, **458**, 97–101.

Maher,C.A. *et al.* (2009) Chimeric transcript discovery by paired-end transcriptome sequencing. *PNAS*, **106**, 12353–12358.

McPherson,A. *et al.* (2011) deFuse: an algorithm for gene fusion discovery in tumor RNA-Seq data. *PLoS Comput. Biol.*, **7**, e1001138.

Quail,M.A. *et al.* (2009) Improved protocols for the illumina genome analyzer sequencing system. *Curr. Prot. Human Genet.*, **18**, 18.2.

Sboner,A. *et al.* (2010) FusionSeq: a modular framework for finding gene fusions by analyzing paired-end RNA-sequencing data. *Genome Biol.*, **11**, R104.

Soverini,S. *et al.* (2011) IDH2 somatic mutations in chronic myeloid leukemia patients in blast crisis. *Leukemia: Off. J. Leukemia Soc. Am.*, **25**, 178–181.

Steidl,C. *et al.* (2011) MHC class II transactivator CIITA is a recurrent gene fusion partner in lymphoid cancers. *Nature*, **471**, 377–381.

Trapnell,C. *et al.* (2009) TopHat: discovering splice junctions with RNA-Seq. *Bioinformatics*, **25**, 1105–1111.

Trapnell,C. *et al.* (2010) Transcript assembly and quantification by RNA-Seq reveals unannotated transcripts and isoform switching during cell differentiation. *Nat. Biotechnol.*, **28**, 511–515.

Wang,K. *et al.* (2010) MapSplice: Accurate mapping of RNA-seq reads for splice junction discovery. *Nucleic Acids Res.*, **38**, e178–e178.